The Journal of Immunology

Dragon (Repulsive Guidance Molecule b) Inhibits IL-6 Expression in Macrophages

Yin Xia, Virna Cortez-Retamozo, Vera Niederkofler, Rishard Salie, Shanzhuo Chen, Tarek A. Samad, Charles C. Hong, Silvia Arber, Jatin M. Vyas, Ralph Weissleder, Mikael J. Pittet and Herbert Y. Lin

J Immunol 2011; 186:1369-1376; Prepublished online 27 December 2010;
doi: 10.4049/jimmunol.1002047
http://www.jimmunol.org/content/186/3/1369

The Journal of Immunology is published twice each month by
The American Association of Immunologists, Inc.,
1451 Rockville Pike, Suite 650, Rockville, MD 20852

Print ISSN: 0022-1767 Online ISSN: 1550-6606.

Dragon (Repulsive Guidance Molecule b) Inhibits IL-6 Expression in Macrophages

Yin Xia,[*,†,‡,1] Virna Cortez-Retamozo,[*] Vera Niederkofler,[§,¶] Rishard Salie,[§,¶] Shanzhuo Chen,[*,†,‡] Tarek A. Samad,[‖] Charles C. Hong,[#,] Silvia Arber,[§,¶] Jatin M. Vyas,[††] Ralph Weissleder,[*,‡‡] Mikael J. Pittet,[*] and Herbert Y. Lin[*,†,‡]**

Repulsive guidance molecule (RGM) family members RGMa, RGMb/Dragon, and RGMc/hemojuvelin were found recently to act as bone morphogenetic protein (BMP) coreceptors that enhance BMP signaling activity. Although our previous studies have shown that hemojuvelin regulates hepcidin expression and iron metabolism through the BMP pathway, the role of the BMP signaling mediated by Dragon remains largely unknown. We have shown previously that Dragon is expressed in neural cells, germ cells, and renal epithelial cells. In this study, we demonstrate that Dragon is highly expressed in macrophages. Studies with RAW264.7 and J774 macrophage cell lines reveal that Dragon negatively regulates IL-6 expression in a BMP ligand-dependent manner via the p38 MAPK and Erk1/2 pathways but not the Smad1/5/8 pathway. We also generated Dragon knockout mice and found that IL-6 is upregulated in macrophages and dendritic cells derived from whole lung tissue of these mice compared with that in respective cells derived from wild-type littermates. These results indicate that Dragon is an important negative regulator of IL-6 expression in immune cells and that Dragon-deficient mice may be a useful model for studying immune and inflammatory disorders. *The Journal of Immunology*, **2011, 186: 1369–1376.**

Bone morphogenetic proteins (BMPs) represent a large subfamily of the TGF-β superfamily of ligands that transduce their signals through type I and II serine/threonine kinase receptors and intracellular Smad proteins. TGF-β superfamily members play numerous roles in physiologic and pathologic processes, including cell proliferation, differentiation, apoptosis, and specification of developmental fate during embryogenesis and in adult tissues (1). TGF-β signaling also regulates immune function as demonstrated by the targeted inactivation of TGF-β1 in mice, which led to a mixed inflammatory cell response and to tissue necrosis (2). Subsequent studies revealed that activins (3, 4) and BMPs (5–11) also regulate inflammatory cytokines and chemokines in various cell types, including macrophages, monocytes, and osteoblastic cells.

Dragon (RGMb), along with two other members of the repulsive guidance molecule (RGM) family, RGMa and RGMc (hemojuvelin), are GPI-linked membrane-associated proteins. Recently, we showed that the three RGM proteins are all coreceptors that enhance BMP signaling through increased utilization of BMP type II receptor ActRIIA by BMP2 and BMP4 (12–18). Dragon is expressed in neural tissues, where it may promote cell–cell adhesion by homophilic interactions (19). Dragon also is expressed in other organs, including the ovary, testis, and kidney (13, 16). In the kidney, Dragon is expressed in the epithelium of renal tubules, where it may facilitate the formation of tight junctions via the BMP–Smad signaling pathway (16). However, the expression and function of Dragon in other cells and organs have not been characterized.

Because BMP signaling can regulate macrophage function, we investigated whether Dragon plays a role in this process. We found that Dragon is highly expressed in macrophages and is involved directly in the suppression of IL-6 expression through the p38 MAPK and Erk1/2 pathways. Through the generation of Dragon knockout (KO) mice, we report a central role of Dragon in controlling IL-6 expression in lung macrophages in vivo. To our knowledge, this is the first BMP signaling function in vivo that has been identified for the Dragon protein.

Materials and Methods

RT-PCR

Total RNA was isolated from RAW264.7 macrophages using an RNeasy mini kit (Qiagen) according to the manufacturer's instructions. First-strand cDNA synthesis was performed using an iScript cDNA synthesis kit (Bio-

*Center for Systems Biology, Massachusetts General Hospital, Harvard Medical School, Boston, MA 02114; [†]Program in Membrane Biology, Massachusetts General Hospital, Harvard Medical School, Boston, MA 02114; [‡]Division of Nephrology, Department of Medicine, Massachusetts General Hospital, Harvard Medical School, Boston, MA 02114; [§]Department of Cell Biology, Biozentrum, University of Basel, Basel, Switzerland; [¶]Friedrich Miescher Institute for Biomedical Research, Basel, Switzerland; [‖]Neural Plasticity Research Unit, Department of Anesthesia, Massachusetts General Hospital, Harvard Medical School, Boston, MA 02114; [#]Research Medicine, Veterans Affairs Tennessee Valley Healthcare System, Nashville, TN 37212; **Division of Cardiovascular Medicine, Vanderbilt University School of Medicine, Nashville, TN 37232; [††]Division of Infectious Disease, Department of Medicine, Massachusetts General Hospital, Harvard Medical School, Boston, MA 02114; and [‡‡]Department of Systems Biology, Harvard Medical School, Boston, MA 02115

[1]Current address: School of Biomedical Sciences, Faculty of Medicine, The Chinese University of Hong Kong, Shatin, N.T., Hong Kong, China.

Received for publication June 18, 2010. Accepted for publication November 23, 2010.

This work was supported by National Institutes of Health Grants R01 DK-071837 and R01 DK-069533 (to H.Y.L.), R03 HD60641 and K01 DK084081 (to Y.X.), and U01 HL080731, P50 CA86355, and U54 CA126515 (to V.C.R., M.J.P., and R.W.).

Address correspondence and reprint requests to Yin Xia or Herbert Y. Lin, Center for Systems Biology, CPZN 8150, Massachusetts General Hospital, 185 Cambridge Street, Boston, MA 02114 (Y.X.) or Center for Systems Biology, CPZN 8216, Massachusetts General Hospital, 185 Cambridge Street, Boston, MA 02114 (H.Y.L.). E-mail addresses: Xia.Yin@mgh.harvard.edu (Y.X.) or Lin.Herbert@mgh.harvard.edu (H.Y.L.)

The online version of this article contains supplemental material.

Abbreviations used in this article: BMP, bone morphogenetic protein; ES, embryonic stem; IMCD3, inner medullar collecting duct; KO, knockout; PASMC, pulmonary artery smooth muscle cell; RGM, repulsive guidance molecule; RT, reverse transcription; siRNA, small interfering RNA; WT, wild-type.

Rad). Transcripts of mouse BMP2, BMP4, BMP5–7, and RGMb were amplified using the primers described previously (14, 16).

Small interfering knockdown

Mouse Dragon and BMPRII small interfering RNAs (siRNAs) were purchased from Ambion, and the sequences were described previously (14). SMARTpool siRNAs against mouse Smad4 were purchased from Dharmacon. siRNA duplexes (100 nM) were added to subconfluent RAW264.7 or J774 macrophages using Lipofectamine 2000 (Invitrogen) or DharmaFectI (Dharmacon). Cells then were incubated with or without BMP4 (50 ng/ml; R&D Systems), LPS (10 ng/ml; Sigma), the p38 MAPK inhibitor SB203580 (2.5 μM), or the Erk1/2 inhibitor PD98059 (2.5 μM). Assays to measure mRNA levels of IL-6, MCP-1, TNF-α, IL-1β, IFN-γ, RGMb, Id1, and RPL19 or phosphorylation levels of Smad1/5/8, p38 MAPK, or Erk1/2 were performed 46 h after transfection. For the experiments with pulmonary artery smooth muscle cells (PASMCs), HUVECs, inner medullar collecting duct (IMCD3) cells, and C2C12 cells, Dragon siRNA duplexes were used at concentrations of 60–80 nM.

Dragon cDNA transfection

Mouse Dragon cDNA (200 ng/ml) was transfected into RAW264.7 macrophages using Lipofectamine 2000. Transfected cells then were incubated with noggin (500 ng/ml; R&D Systems) or LDN-193189 (0, 40, and 400 ng/ml; Shanghai United Pharmatech Company, Shanghai, China). Assays to measure mRNA levels of IL-6 and RPL19 were performed 46 h after transfection.

Measurement of gene expression

Real-time quantification of mRNA transcripts was performed as described previously (14, 15). First-strand cDNA was amplified with the primers as described previously (9, 14, 20, 21). Results are expressed as a ratio of the gene of interest to RPL19.

Western blotting

Lung tissues or RAW264.7 cells were lysed in TBS (50 mM Tris-HCl, 150 mM NaCl, and 1% Triton X-100 [pH 7.4]) containing protease inhibitor mixture (Pierce) and phosphatase inhibitor mixture (Pierce) for 30 min on ice. After centrifugation for 10 min at 4°C, the supernatant was assayed for protein concentration by colorimetric assay (BCA kit; Pierce). A total of 20–40 μg of protein was separated by SDS-PAGE and transferred to polyvinylidene difluoride membranes. Membranes were probed with rabbit anti–phospho-Smad1/5/8, anti–phospho-p38 MAPK, and anti–phospho-Erk1/2 polyclonal Abs (1:1000 dilution; Cell Signaling Technology, Beverly, MA) or goat anti-mouse IL-6 (R&D Systems). Membranes were stripped in 0.2 M glycine (pH 2.5) and 0.5% Tween 20 for 10 min and reprobed with rabbit anti-Smad1, anti-total p38 MAPK, anti-total Erk1/2 (Cell Signaling), or anti-actin Abs (Sigma).

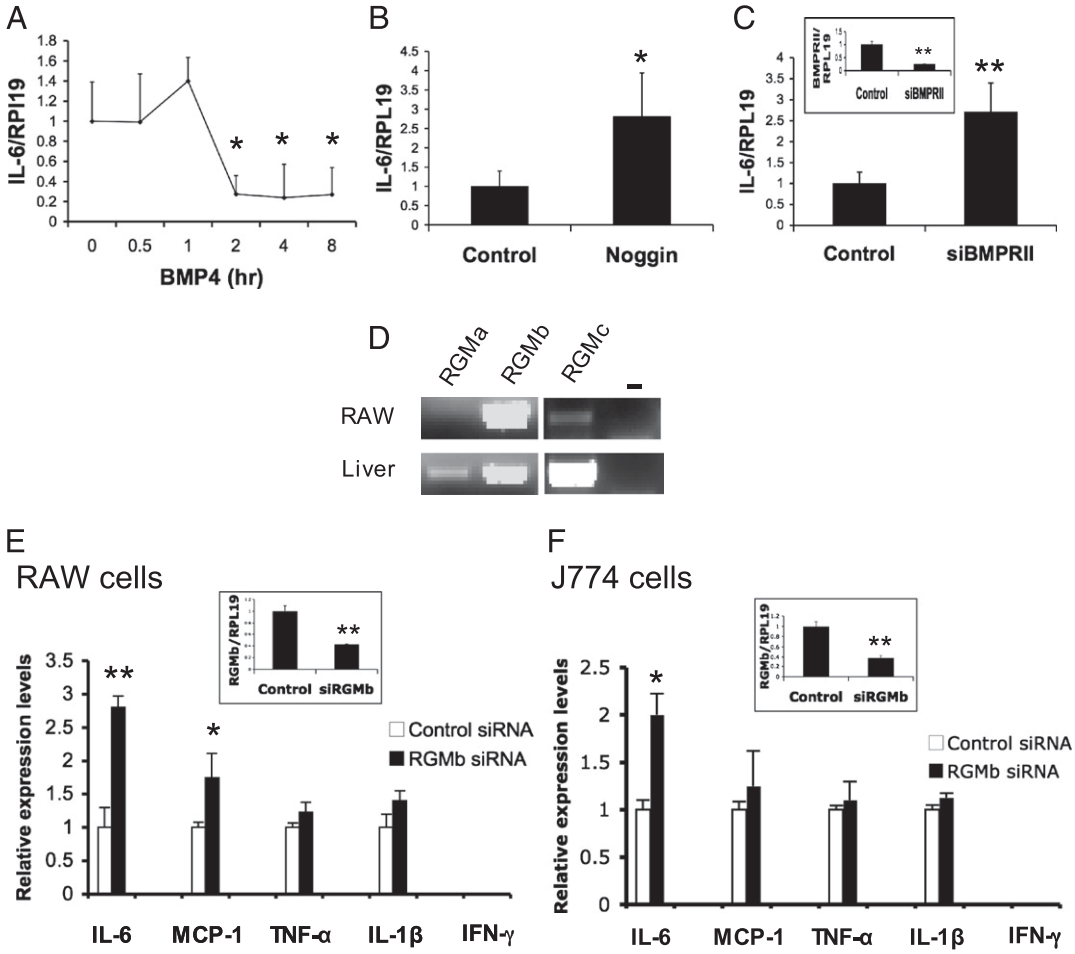

FIGURE 1. IL-6 is a target of Dragon in RAW264.7 and J774 macrophages. *A–C*, IL-6 mRNA expression is inhibited by BMP4 (*A*) and increased by noggin (*B*) or by inhibition of BMPRII expression (*C*). RAW264.7 macrophages were incubated with BMP4 (50 ng/ml) for 0–8 h, incubated with noggin (500 ng/ml) overnight, or transfected with control or BMPRII siRNA. Cells then were harvested for RNA extraction and real-time PCR for IL-6 and RPL19. IL-6 expression levels of the treated cells were expressed as a fraction of values from the controls. *D*, Expression of RGMa, RGMb, and RGMc mRNAs in RAW264.7 macrophages. Total RNA from RAW264.7 cells was extracted for RT-PCR to determine the expression of RGMa, RGMb, and RGMc. Total RNA from the mouse liver was used in PCR analyses as positive controls. *E* and *F*, IL-6 mRNA expression is upregulated by inhibition of Dragon expression in RAW264.7 (*E*) and J774 (*F*) macrophages. RAW264.7 (*E*) or J774 (*F*) cells were transfected with control or Dragon siRNA and analyzed for mRNA levels of IL-6, MCP-1, TNF-α, IL-1β, IFN-γ, and Dragon. The expression levels of these factors are normalized to RPL19 and expressed as a fraction of values from the respective controls. The efficacy of BMPRII siRNA or Dragon siRNA is shown in the insets. $*p < 0.05$; $**p < 0.01$.

Dragon KO mice

To generate Dragon KO mice (C57/B6/129), a mouse genomic library was screened using a mRGMb-specific probe (Incyte Genomics, Palo Alto, CA). The second coding exon of mRGMb was disrupted by inserting a cassette containing an enhanced GFP, followed by an IRES-NLS-LacZ-pA and a thymidine kinase-neomycin cassette using homologous recombination in embryonic stem (ES) cells. ES cell recombinants were screened by Southern blot analyses. The genotyping of mRGMb mutant mice was performed by Southern blotting (primers for the probe, 5′-GTT CCT AGG GAG AAT AGC GTC TCC-3′ and 5′-ACA GGC ACG TTC GTC ACT TGA ACC-3′) (Supplemental Fig. 4) or PCR (5′-GTC AAT CCG CCG TTT GTT CCC ACG G-3′ and 5′-GCG TGT ACC ACA GCG GAT GGT TCG G-3′ for the KO allele; 5′-ACA GGC ACG TTC GTC ACT TGA ACC-3′ and 5′-GTT CCT AGG GAG AAT AGC GTC TCC-3′ for the wild-type [WT] allele). Northern blot and RT-PCR analyses of mRGMb KO mice confirmed the absence of RGMb mRNA in the brain and lung, respectively (Supplemental Fig. 4). A sequence described previously for in situ hybridization was used for the probe for Northern blot analysis (22).

Mice were housed under specific pathogen-free conditions with a light/dark cycle of 12 h/12 h and ad libitum access to food and water. Heterozygous animals were bred to obtain homozygous Dragon-null mice. All of the procedures were performed in accordance with Massachusetts General Hospital animal care regulations.

Flow cytometry

Mice were sacrificed 10–12 d after birth. Lungs were digested with collagenase I (Sigma-Aldrich) at 37°C for 1 h. RBCs were lysed with ammonium chloride potassium lysis buffer. The cells were washed and resuspended in HBSS supplemented with 0.2% (w/v) BSA and 1% (w/v) FCS. The total number of living cells was determined with trypan blue (Mediatech).

Cell suspensions were incubated with a mixture of mAbs against T cells (CD90-PE, 53-2.1), B cells (B220-PE, RA3-6B2), NK cells (CD49b-PE, DX5; NK1.1-PE, PK136), granulocytes (Ly-6G-PE, 1A8), myeloid cells (CD11b-allophycocyanin, M1/70), and monocyte subsets (Ly-6C-FITC, AL-21) (BD Biosciences). Monocytes were identified as $CD11b^{high}$ (CD90/B220/CD49b/NK1.1/Ly-6G)^{low} (F4/80/CD11c)^{low} Ly-$6C^{high/low}$; macrophages as $F4/80^{high}$ ($CD11b^{low}$); dendritic cells (DCs) as $CD11c^{high}$ $CD11b^{high}$; and neutrophils as $CD11b^{high}$ Ly-$6G^{high}$. Reported cell numbers were calculated as the product of the total number of living cells and the percentage of cells within their respective gates. Data were acquired on a LSRII (BD Biosciences) and analyzed with FlowJo, version 8.5.2 (Tree Star). For gene expression analysis, the cells mentioned above were sorted with a FACSAria II (BD Biosciences) into 250 μl RLT buffer, and total RNA was extracted using an RNeasy mini kit.

Data analysis

The results are presented as the mean ± SD of three determinations from two or three independent experiments for the in vitro studies or the mean ± SD of 6–7 mice (Fig. 6*A–C*), 6 mice (Fig. 7*A*), 3–4 mice (Fig. 7*B*), or 4–6 mice (Supplemental Fig. 7) for the in vivo studies. Dragon expression levels in different cell populations in the lung of WT mice were analyzed by one-way ANOVA. Other differences were assessed by Student *t* test. Differences of $p < 0.05$ were considered significant.

Results

Dragon suppresses IL-6 expression through a BMP ligand-dependent pathway

It has been shown that BMP signaling inhibits IL-6 expression in a number of cell types, including macrophages (5–7, 9). Consistent with these previous findings, BMP4 inhibited IL-6 mRNA expression in RAW264.7 macrophages (Fig. 1*A*). The inhibition was seen as early as 2 h after exogenous BMP4 treatment (Fig. 1*A*). Incubation with noggin, an extracellular antagonist of BMP ligands (Fig. 1*B*) or inhibition of BMP type II receptor BMPRII expression by siRNA increased IL-6 mRNA expression (Fig. 1*C*).

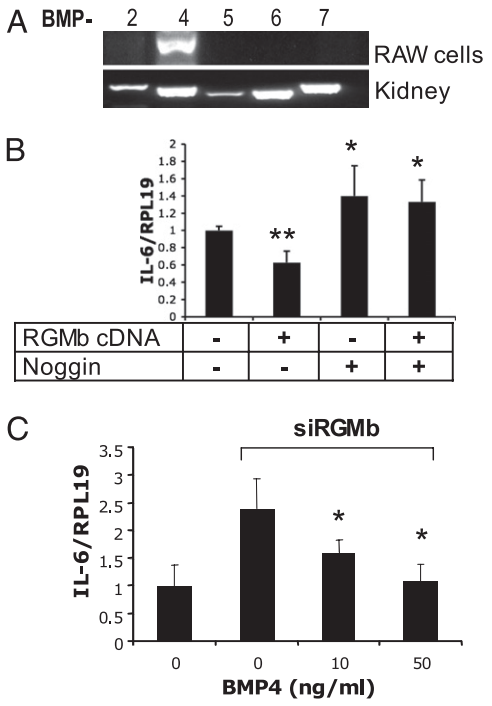

FIGURE 2. Dragon action on IL-6 expression is BMP ligand-dependent. *A*, Expression of BMP ligands BMP2 and BMP4–BMP7 in RAW264.7 macrophages. Total RNA from RAW cells was extracted for RT-PCR to determine the expression of BMP2 and BMP4–BMP7 mRNAs. Total RNA from the mouse kidney was used in PCR analyses as positive controls. *B*, Inactivation of BMP ligands by noggin abolished inhibition of IL-6 expression induced by RGMb overexpression. RAW264.7 cells was transfected with and without Dragon cDNA, followed by incubation with and without noggin (500 ng/ml). The cells then were harvested for real-time PCR analysis of IL-6 and RPL19 mRNA levels. *C*, Induction of IL-6 expression by inhibition of RGMb expression was attenuated by exogenous BMP4. RAW264.7 cells were transfected with and without Dragon siRNA, and the cells transfected with Dragon siRNA were incubated with increasing amounts of BMP4 (0–50 ng/ml). The cells then were harvested for real-time PCR analysis for IL-6 and RPL19 mRNA levels. $*p < 0.05$; $**p < 0.01$ versus the controls (bar 1 in *B* and bar 2 in *C*).

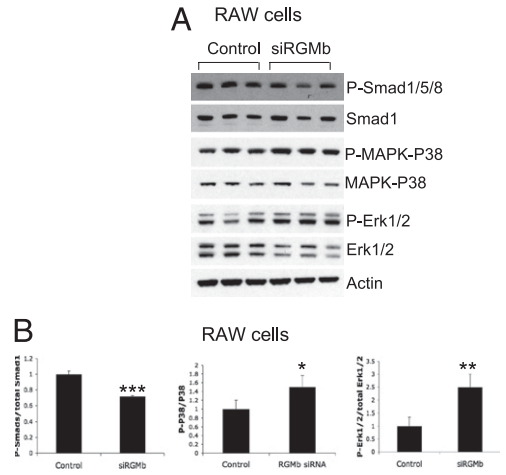

FIGURE 3. Changes in phosphorylation levels of Smad1/5/8, p38 MAPK, and Erk1/2 in Dragon knockdown RAW264.7 cells. *A*, RAW264.7 cells were transfected with control (three replicates) and Dragon siRNA (three replicates). Forty-six hours after transfection, the cells were lysed and analyzed by Western blotting for phospho-Smad1/5/8 and total Smad1; phospho-p38 MAPK and total p38 MAPK; phospho-Erk1/2 and total Erk1/2; and actin. *B*, Western blot chemiluminescence from experiments in *A* was quantified using IPLab Spectrum software for phospho-Smad1/5/8 relative to Smad1, phospho-p38 MAPK relative to total p38 MAPK, and phospho-Erk1/2 relative to total Erk1/2. $*p < 0.05$; $**p < 0.01$; $***p < 0.001$.

These results confirm the previously published findings that BMP signaling inhibits IL-6 expression in macrophages in vitro (5, 6).

We have shown previously that Dragon is a coreceptor that enhances BMP signaling (12, 13, 16). To examine whether Dragon regulates IL-6 expression in macrophages, we first examined the expression of Dragon in RAW264.7 cells. As shown by RT-PCR, Dragon mRNA was highly expressed in RAW264.7 cells, whereas the expression of two other members of the RGM family was either weak (RGMc) or undetectable (RGMa) (Fig. 1*D*). Inhibition of Dragon expression by siRNA increased basal IL-6 mRNA levels by 2.8-fold (Fig. 1*E*). Inhibition of Dragon expression only modestly increased MCP-1 expression and did not alter the expression of TNF-α and IL-1β (Fig. 1*E*). A selective increase in IL-6 expression by inhibition of Dragon also was observed in J774 macrophages (Fig. 1*F*). In addition, inhibition of Dragon expression in RAW264.7 cells increased LPS-stimulated IL-6 mRNA levels by 1.8-fold, whereas MCP-1, TNF-α, and IL-1β mRNA levels did not change (Supplemental Fig. 1). These results suggest that IL-6 is an important cytokine target of Dragon action in macrophages.

IL-6 and Dragon mRNAs also were expressed in mouse PASMCs, HUVECs, mouse IMCD3 cells, and C2C12 mouse myoblasts. Inhibition of Dragon mRNA by 70–90% did not alter IL-6 expression in PASMCs, HUVECs, and IMCD3 cells and slightly increased IL-6 expression in C2C12 cells (Supplemental Fig. 2). These results suggest that the action of Dragon in IL-6 expression is specific for macrophage cell types.

Our previous studies have shown that Dragon.Fc binds to radiolabeled BMP2 and BMP4 and that BMP signaling induced by transfected Dragon was reduced after inhibition of BMP4 expression in IMCD3 cells, suggesting that BMP2 and BMP4 are the endogenous BMP ligand for the Dragon coreceptor (12, 16). To examine whether the ability of Dragon to inhibit IL-6 expression is dependent on BMP ligands, we examined the expression of BMP2, BMP4, and the closely related BMP5, BMP6, and BMP7 (Fig. 2*A*) in RAW264.7 macrophages. BMP4 mRNA was detected, whereas while BMP2, BMP5, BMP6, and BMP7 were not. Transfection of RAW264.7 cells with Dragon cDNA inhibited IL-6 expression, whereas addition of noggin abolished this inhibition (Fig. 2*B*). Silencing of Dragon induced IL-6 expression, whereas exogenous

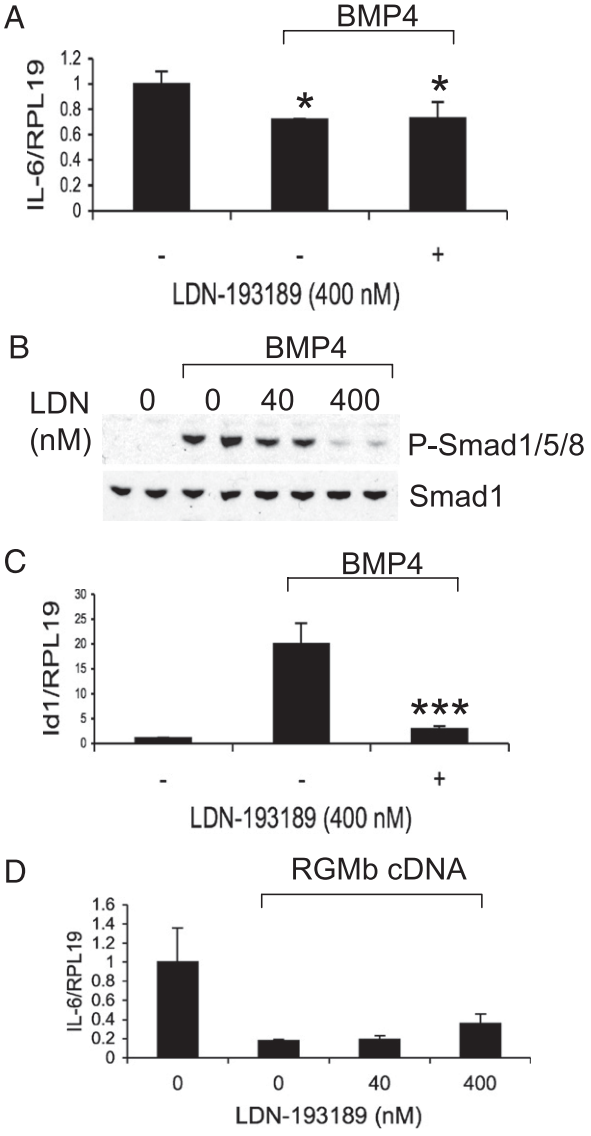

FIGURE 4. Inhibition of IL-6 expression by BMP4 and Dragon is not affected by LDN-193189. *A*, RAW264.7 cells were treated with or without BMP4 (50 ng/ml) in the presence or absence of LDN-193189 (400 nM). The cells then were harvested for real-time PCR analysis for IL-6 and RPL19 mRNA levels. *B*, RAW264.7 cells were treated with or without BMP4 (50 ng/ml) in the presence of increasing amounts of LDN-193189 (0–400 nM). The cells were lysed and analyzed by Western blotting for phospho-Smad1/5/8 and total Smad1. *C*, RAW264.7 cells were treated with or without BMP4 (50 ng/ml) in the presence or absence of LDN-193189 (400 nM). The cells then were harvested for real-time PCR analysis for Id1 mRNA levels. *D*, RAW264.7 cells were transfected with or without Dragon cDNA. The cells transfected with Dragon cDNA then were treated with increasing amounts of LDN-193189 (0–400 nM). The cells were harvested for real-time PCR analysis for IL-6 and RPL19 mRNA levels. $*p < 0.05$; $***p < 0.001$ versus cells treated with BMP4 in the absence of LDN-193189 (bar 2, *C*).

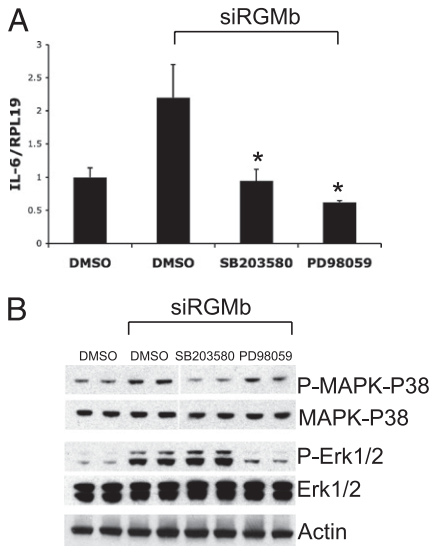

FIGURE 5. Induction of IL-6 expression by Dragon siRNA is abolished by p38 MAPK inhibitor SB203580 or Erk1/2 inhibitor PD98059. *A*, RAW264.7 cells were transfected with control or Dragon siRNA, followed by incubation with DMSO, SB203580 (2.5 μM), or PD98059 (2.5 μM). The cells were analyzed by real-time PCR for IL-6 and RPL19 mRNA levels. *B*, RAW264.7 cells were transfected with control or Dragon siRNA, followed by incubation with DMSO, SB203580 (2.5 μM), or PD98059 (2.5 μM). The cells were lysed and analyzed by Western blotting for phospho-p38 MAPK and total p38 MAPK; and phospho-Erk1/2 and total Erk1/2. $*p < 0.05$ versus cells transfected with Dragon siRNA in the absence of any inhibitors (bar 2).

BMP4 addition abolished this induction (Fig. 2*C*). These results suggest that endogenous BMP ligand(s) is required for Dragon to inhibit IL-6 expression.

The action of Dragon in IL-6 expression is mediated by the p38 MAPK and Erk1/2 pathways but not the Smad1/5/8 pathway

To explore the mechanisms involved in the regulation of IL-6 expression by Dragon, we examined the effects on the Smad1/5/8, p38 MAPK, and Erk1/2 pathways, which are well-documented pathways that mediate BMP actions (1). As shown in Fig. 3*A* and 3*B*, phospho-Smad1/5/8 levels were decreased, but phospho-p38 MAPK and phospho-Erk1/2 levels were increased, after inhibition of Dragon expression by siRNA. To examine whether the Smad pathway plays a role in the regulation of IL-6 expression by BMP4 and Dragon, we used LDN-193189, a small molecule BMP inhibitor, which inhibits Smad1/5/8 phosphorylation but does not affect p38 MAPK and Erk1/2 activity (16, 23). LDN-193189 treatment did not affect the inhibition of IL-6 expression induced by BMP4 (Fig. 4*A*). In contrast, the induction of phospho-Smad1/5/8 levels and Id1 expression by BMP4 was reduced dramatically by LDN-193189 (Fig. 4*B*, 4*C*). LDN-193189 treatment also did not affect the inhibition of IL-6 expression induced by Dragon (Fig. 4*D*). Finally, inhibition of Smad4 expression by siRNA did not affect IL-6 mRNA levels, although it significantly reduced Id1 mRNA expression in RAW264.7 cells (Supplemental Fig. 3). These results suggest that regulation of IL-6 by Dragon/BMP does not involve the Smad pathway.

To examine whether the p38 MAPK and Erk1/2 pathways are involved in the regulation of IL-6 expression by Dragon, we used p38 MAPK inhibitor SB203580 or Erk1/2 inhibitor PD98059. IL-6 expression induced by Dragon siRNA was abolished by treatment with SB203580 or PD98059 (Fig. 5*A*), which, respectively, reduced phospho-p38 MAPK and phospho-Erk1/2 protein levels that were induced when Dragon was inhibited (Fig. 5*B*). These results suggest that p38 MAPK and Erk1/2 mediate the action of Dragon on lowering IL-6 mRNA levels.

IL-6 expression is upregulated in the lungs and livers of Dragon KO mice

To examine if Dragon plays a role in regulating IL-6 expression in vivo, we analyzed IL-6 expression in the lungs, livers, spleens, colons, and muscles of Dragon KO mice. Dragon KO mice were generated using gene targeting in ES cells by homologous recombination (Supplemental Fig. 4). Because Dragon KO mice die 2–3 wk after birth (cause of mortality under investigation), we collected samples from Dragon KO and WT littermates at 10–12 d of age. As shown in Fig. 6*A*, IL-6 mRNA expression was upregulated by 10-fold in the lungs of KO mice compared with that in the WT mice. IL-6 protein also was upregulated, as shown by Western blot analysis (Fig. 6*D*). IL-6 mRNA levels were significantly higher in E20.5 KO lungs than those in E20.5 WT lungs (Fig. 6*B*). IL-6 mRNA levels were 2.9-fold higher in KO livers than those in WT livers of 10- to 12-d-old mice (Fig. 6*C*). IL-6 mRNA expression was 16-fold lower in the spleen, colon, and

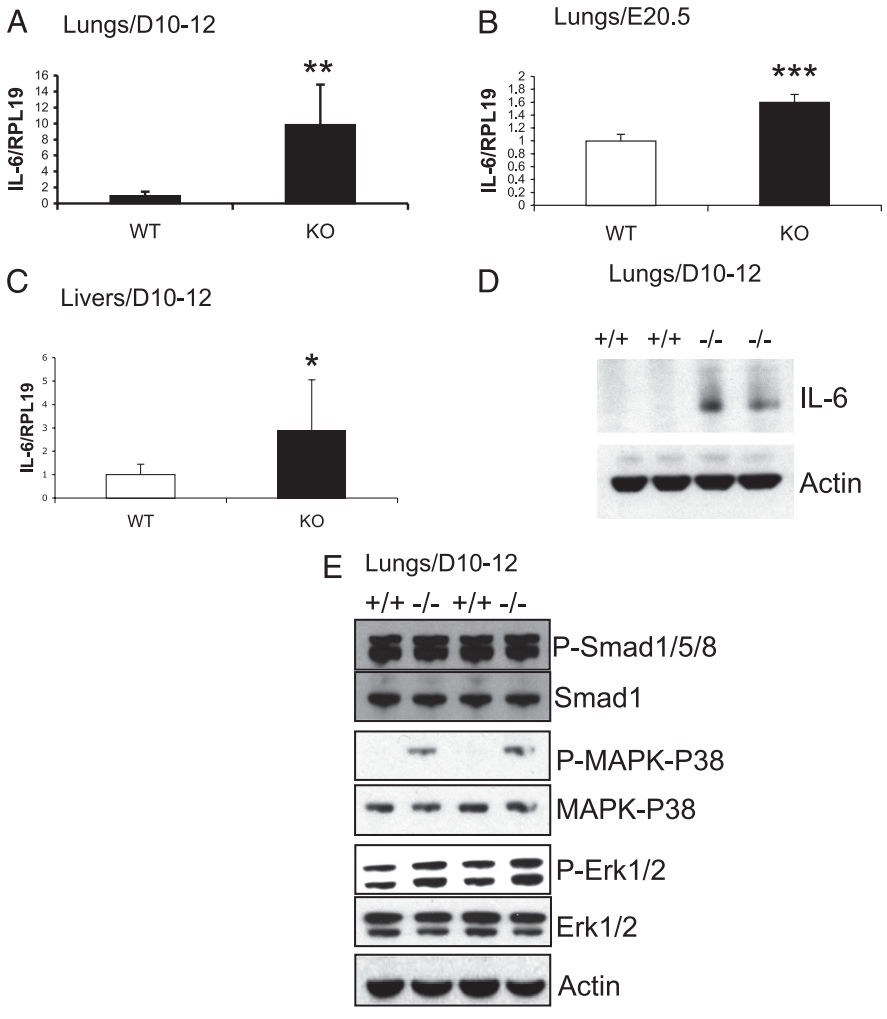

FIGURE 6. IL-6 mRNA expression is upregulated in the lung and liver of Dragon KO mice and embryos. *A–C*, Total RNA was extracted from lungs (*A*) and livers (*C*) of WT and Dragon KO mice at 10–12 d of age or from lungs (*B*) of E20.5 WT and Dragon KO fetuses. mRNA levels were measured by quantitative real-time PCR, were normalized to RPL19 mRNA levels, and are expressed as a fraction of values from WT samples. *D*, IL-6 protein is upregulated in the lung of Dragon KO mice. Lysates from lungs of 10- to 12-d-old WT (+/+) and Dragon KO (−/−) mice were subjected to Western blot analysis for IL-6. The membrane was stripped and probed with actin Abs. *E*, Changes in phosphorylation levels of Smad1/5/8, p38 MAPK, and Erk1/2 in Dragon KO lungs. Lysates from lungs of 10- to 12-d-old WT (+/+) and Dragon KO (−/−) mice were subjected to Western blot analysis for phospho-Smad1/5/8, phospho-p38 MAPK, and phospho-Erk1/2. The membranes were stripped and probed with total Smad1, p38 MAPK, and Erk1/2 Abs, respectively. $*p < 0.05$; $**p < 0.01$; $***p < 0.001$ versus WT. $n = 6–7$.

muscle compared with the IL-6 levels in the lung of 10- to 12-d-old WT mice (data not shown), and IL-6 mRNA levels in these organs were not altered between KO and WT mice (Supplemental Fig. 5). In addition to IL-6, a number of other inflammatory cytokines and chemokines, including MCP-1, TNF-α, IL-1β, and IFN-γ, also were upregulated in the lung of Dragon KO mice at 10–12 d after birth (Supplemental Fig. 6). These results suggest that Dragon is a negative regulator of IL-6 and other inflammatory factors in the lung and liver in vivo.

In the lungs of Dragon KO mice, phospho-Smad1/5/8 levels did not change, whereas phospho-p38 MAPK and phospho-Erk1/2 levels in KO lungs were increased compared with those in WT lungs (Fig. 6*E*). These results are consistent with the in vitro observation in cultured RAW264.7 cells that Dragon acts through the p38 MAPK and Erk1/2 pathways, but not the Smad1/5/8 pathway, to regulate IL-6 expression.

IL-6 mRNA is upregulated in macrophages in the lungs of Dragon KO mice

Next, we sought to characterize which cells increase IL-6 expression in the lungs of Dragon KO mice. To this end, we purified and analyzed diverse populations of the tissue immune cell repertoire from 10- to 12-d-old WT and Dragon KO mice (Fig. 7, Supplemental Fig. 7). The total number of cells in the lung was similar between WT and Dragon KO mice. The numbers of Ly-6C^{high} and Ly-6C^{low} monocytes, macrophages, DCs, and neutrophils were not significantly different between the two genotypes (Supplemental Fig. 7).

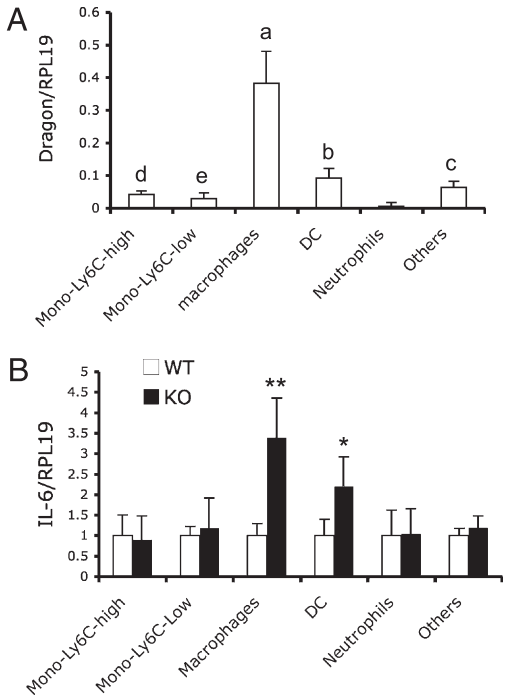

FIGURE 7. Dragon mRNA expression in Ly-6C^{high} and Ly-6C^{low} monocytes, macrophages, DCs and neutrophils in lungs of 10- to 12-d-old WT mice (*A*), and IL-6 mRNA expression in the five cell populations and the rest of the cells (others) in WT and KO mice (*B*). Total RNA was extracted from sorted Ly-6C^{high} and Ly-6C^{low} monocytes, macrophages, DCs, neutrophils, and other cells in lungs of 10- to 12-d-old WT and KO mice. Real-time PCR analyses were performed to quantify Dragon and IL-6 mRNA levels. RPL-19 was used as an internal control. ^{abcde}Values with different superscripts differ significantly; $*p < 0.05$; $**p < 0.01$ (*B*). $n = 6$ (*A*) or 3–4 (*B*).

Dragon mRNA was expressed in Ly-6C^{high} and Ly-6C^{low} monocytes, macrophages, and DCs, although it is barely detectable in neutrophils collected from lungs of 10- to 12-d-old WT mice (Fig. 7*A*). Dragon expression was much higher in macrophages than that in Ly-6C^{high} and Ly-6C^{low} monocytes, DCs, neutrophils, and other cells, with Dragon expression being higher in DCs than that in monocytes, neutrophils, and other cells (Fig. 7*A*). IL-6 mRNA expression was increased by 3.4-fold in macrophages and 2.2-fold in DCs due to Dragon deletion, while no changes in IL-6 mRNA levels were observed in Ly-6C^{high} and Ly-6C^{low} monocytes, neutrophils, and other cells (Fig. 7*B*). These results suggest that high levels of Dragon in lung macrophages (and DCs) serve to suppress IL-6 expression in vivo, which are consistent with our in vitro data.

Discussion

The three RGM family members RGMa, RGMb (Dragon), and RGMc (hemojuvelin) are BMP coreceptors that enhance BMP signaling. Our published studies have shown that RGMc/hemojuvelin acts through the BMP pathway to regulate hepcidin expression and iron metabolism, but the biological actions of the BMP signaling functions of RGMa and RGMb/Dragon are poorly characterized. Previous studies have shown that BMPs (5, 6, 9) regulate inflammatory cytokines and chemokines, including IL-6, in various cell types, including macrophages and monocytes. In the current study, we confirmed that BMP4 inhibited IL-6 expression in RAW264.7 macrophages. Interestingly, inhibition of Dragon expression in RAW264.7 or J774 macrophages increased IL-6 expression, whereas Dragon overexpression inhibited IL-6 expression in a BMP ligand-dependent manner. These results suggest that Dragon regulates IL-6 expression via the BMP pathway in RAW264.7 macrophages. Inhibition of Dragon expression did not have significant effects on IL-6 expression in PASMCs, HUVECs, mIMCD3, and C2C12 cells. These cells have been shown be responsive to BMP ligands by ourselves and others (9, 14, 16, 24–26). For example, inhibition of BMPRII expression increased IL-6 expression in PASMCs derived from mouse (data not shown) and human (9). Thus, the IL-6 effect of Dragon appears to be specific for macrophages. The reason for this cell type-specific action is unclear.

Our study also demonstrated that Dragon action on IL-6 expression is mediated by the p38 MAPK and Erk1/2 pathways but not by the Smad1/5/8 pathway. Our data show that 1) phosphorylation levels of p38 MAPK and Erk1/2 were increased by inhibition of Dragon expression in vitro and by deletion of Dragon

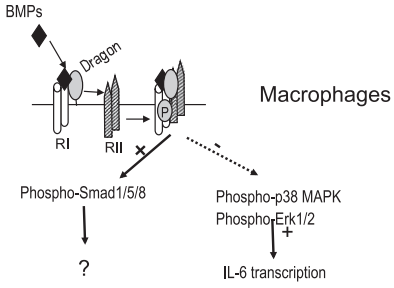

FIGURE 8. Schematic diagram depicting Dragon action in regulating IL-6 expression in macrophages. Dragon/BMPs inhibit phosphorylation of p38 MAPK and Erk1/2 via a mechanism yet to be determined and then suppress IL-6 transcription. Dragon also facilitates BMP ligands to activate Smad1/5/8 through BMP type II and BMP type I receptors, but the biological functions of this activation remain unknown. R I, BMP type I receptors; R II, BMP type II receptors.

in vivo, whereas phosphorylation levels of Smad1/5/8 were reduced by inhibition of Dragon in vitro but not affected by deletion of Dragon in vivo; 2) the induction of IL-6 expression by inhibition of Dragon expression is blocked by a p38 MAPK- or Erk1/2-specific inhibitor; and 3) inhibition of IL-6 expression by exogenous Dragon or BMP4 was not affected by LDN-193189, and IL-6 expression was not affected by inhibition of Smad4 expression. A study by Hagen et al. (9) showed that inhibition of BMPRII in mouse PASMCs also led to increased p38 MAPK activity resulting in increased IL-6 expression. These results suggest an inhibitory effect of BMP2 signaling on p38 MAPK and Erk1/2 activation in these cells. In contrast, previous studies have shown a stimulatory effect of BMP2 on p38 MAPK and Erk1/2 activation in other cell types (27). To add more complexity, a recent study demonstrated that BMP6 and BMP7 suppressed estrogen-induced p38 MAPK and Erk1/2 activation, whereas BMP2 and BMP4 enhanced this stimulation in MCF-7 cells (28). Therefore, whether BMP signaling leads to stimulation or inhibition of the p38 MAPK and Erk1/2 pathways appears to be dependent on the specific BMP ligands and cell types studied.

Previous studies have shown that BMP receptors oligomerize in at least two different manners. BMP type I and type II receptors can form hetero-oligomeric complexes prior to ligand binding. BMPs bind to these preformed hetero-oligomeric complexes and then activate the Smad signaling pathway. The other alternative is that BMP ligand binds to BMP type I receptors and then recruits BMP type II receptors into a complex (BMP-induced signaling complexes), thus activating XIAP-Tak1-Tab1 complex and downstream p38 MAPK and Erk1/2 pathways (27, 29). BMP type I and type II receptors partially reside in lipid rafts. The non-Smad signaling induced by BMP2 depends on the association of BMP receptors with rafts and caveolae, whereas the Smad pathway is independent of lipid raft association (27). Interestingly, Dragon also is localized in lipid rafts (13). Whether Dragon is involved in regulating the formation of BMP-induced signaling complexes and activation of XIAP and TAK1 remains to be investigated.

We found that IL-6 expression was increased dramatically in lung macrophages and DCs as well as in whole lung and liver tissues in the Dragon KO mice compared with that in WT mice. These results revealed an important physiologic role of Dragon in regulating IL-6 expression. The magnitude of the increase in IL-6 mRNA levels in the whole lungs (10-fold) was larger than those in macrophages (3.4-fold) and in DCs (2.2-fold). The reason for the differences between the whole organ and specific cell populations remains unclear, but the cells were analyzed for mRNA levels a few hours after the cells were collected due to the preparation time required for FACS procedures, and IL-6 mRNA expression may have declined during this period of time. IL-6 expression in cells other than monocytes, macrophages, DCs, and neutrophils in the lung was not altered by Dragon deletion. This result is consistent with our in vitro data showing that inhibition of Dragon did not change IL-6 expression in PASMCs, a cell type in the lung, which is involved in mechanisms of disorders, such as pulmonary arterial hypertension, with elevated IL-6 expression.

Expression levels of other factors, including MCP-1, TNF-α, IL-1β, and IFN-γ, also were elevated in the lungs of Dragon KO mice. Our in vitro data using RAW264.7 and J774 cells show that IL-6 is a direct target of the Dragon–BMP pathway, whereas expression of MCP-1, TNF-α, and IL-1β were not affected appreciably by inhibition of Dragon expression. Therefore, the changes in these factors in Dragon KO mice might be due to secondary effects of Dragon/BMP action.

We characterized the Dragon expression profile in five immune cell populations isolated from the lungs of 10- to 12-d-old mice and found that Dragon is expressed most highly in macrophages and DCs and lower in other cell types. This increased expression of Dragon in macrophages and DCs likely accounts for why these cell types dramatically increased their IL-6 expression in the Dragon KO mice compared with that in the WT mice, whereas there was no change in IL-6 expression in Ly-6C^{high} and Ly-6C^{low} monocytes, neutrophils, and other cells.

The growth of Dragon KO mice was retarded (data not shown), and the mice die between 2 and 3 wk after birth. Our preliminary results show that the Dragon KO mice developed growth hormone resistance in the liver and skeletal muscle (data not shown). Growth hormone resistance has been reported in other mice injected with exogenous IL-6 (30) or in mice with transgenic overexpression of IL-6 (31, 32). Therefore, in the future, it will be interesting to investigate whether abnormal expression of IL-6 and other inflammatory factors contribute to the retarded growth and even the mortality of Dragon KO mice.

Dragon has an ability to promote cell–cell adhesion by homophilic interactions (19). Whether this property of Dragon contributes to the difference in migration and other functions among different immune cell populations has not yet been addressed.

In summary, we have demonstrated, to our knowledge, the first in vivo biological role for the BMP signaling function of Dragon, which is that Dragon suppresses IL-6 expression in macrophages. Dragon is most highly expressed in macrophages compared with other immune cells in the lung, and deletion of Dragon in mice leads to increased expression of IL-6 and other inflammatory factors in macrophages and DCs as well as in the lung and the liver. Our results also show that the Dragon–BMP pathway inhibits p38 MAPK and Erk1/2 phosphorylation, thus suppressing IL-6 expression in macrophages. Dragon enhances Smad1/5/8 phosphorylation in macrophages, but the biological consequences of this activation are yet to be determined (Fig. 8). Taken together, our study suggests that Dragon plays an important role in regulating the immune system.

Acknowledgments

We thank Dr. Paul Yu and Dr. Hideyuki Beppu for the mouse PASMCs, Dr. Chia Chi Sun for reading the manuscript, and Dr. Jinzhong Qin and Dr. Fang Wang for helpful discussions.

Disclosures

The authors have no financial conflicts of interest.

References

1. Shi, Y., and J. Massagué. 2003. Mechanisms of TGF-β signaling from cell membrane to the nucleus. *Cell* 113: 685–700.
2. Shull, M. M., I. Ormsby, A. B. Kier, S. Pawlowski, R. J. Diebold, M. Yin, R. Allen, C. Sidman, G. Proetzel, D. Calvin, et al. 1992. Targeted disruption of the mouse transforming growth factor-beta 1 gene results in multifocal inflammatory disease. *Nature* 359: 693–699.
3. Xia, Y., and A. L. Schneyer. 2009. The biology of activin: recent advances in structure, regulation and function. *J. Endocrinol.* 202: 1–12.
4. Vallet, S., S. Mukherjee, N. Vaghela, T. Hideshima, M. Fulciniti, S. Pozzi, L. Santo, D. Cirstea, K. Patel, A. R. Sohani, et al. 2010. Activin A promotes multiple myeloma-induced osteolysis and is a promising target for myeloma bone disease. *Proc. Natl. Acad. Sci. USA* 107: 5124–5129.
5. Gould, S. E., M. Day, S. S. Jones, and H. Dorai. 2002. BMP-7 regulates chemokine, cytokine, and hemodynamic gene expression in proximal tubule cells. *Kidney Int.* 61: 51–60.
6. Lee, M. J., C. W. Yang, D. C. Jin, Y. S. Chang, B. K. Bang, and Y. S. Kim. 2003. Bone morphogenetic protein-7 inhibits constitutive and interleukin-1 β-induced monocyte chemoattractant protein-1 expression in human mesangial cells: role for JNK/AP-1 pathway. *J. Immunol.* 170: 2557–2563.
7. Maric, I., L. Poljak, S. Zoricic, D. Bobinac, D. Bosukonda, K. T. Sampath, and S. Vukicevic. 2003. Bone morphogenetic protein-7 reduces the severity of colon tissue damage and accelerates the healing of inflammatory bowel disease in rats. *J. Cell. Physiol.* 196: 258–264.

8. Hori, M., H. Sawai, Y. Tsuji, H. Okamura, and K. Koyama. 2006. Bone morphogenetic protein-2 counterregulates interleukin-18 mRNA and protein in MC3T3-E1 mouse osteoblastic cells. *Connect. Tissue Res.* 47: 124–132.
9. Hagen, M., K. Fagan, W. Steudel, M. Carr, K. Lane, D. M. Rodman, and J. West. 2007. Interaction of interleukin-6 and the BMP pathway in pulmonary smooth muscle. *Am. J. Physiol. Lung Cell. Mol. Physiol.* 292: L1473–L1479.
10. Kwon, S. J., G. T. Lee, J. H. Lee, W. J. Kim, and I. Y. Kim. 2009. Bone morphogenetic protein-6 induces the expression of inducible nitric oxide synthase in macrophages. *Immunology* 128(1, Suppl.): e758–e765.
11. Hong, J. H., G. T. Lee, J. H. Lee, S. J. Kwon, S. H. Park, S. J. Kim, and I. Y. Kim. 2009. Effect of bone morphogenetic protein-6 on macrophages. *Immunology* 128 (1, Suppl.): e442–e450.
12. Samad, T. A., A. Rebbapragada, E. Bell, Y. Zhang, Y. Sidis, S. J. Jeong, J. A. Campagna, S. Perusini, D. A. Fabrizio, A. L. Schneyer, et al. 2005. DRAGON, a bone morphogenetic protein co-receptor. *J. Biol. Chem.* 280: 14122–14129.
13. Xia, Y., Y. Sidis, A. Mukherjee, T. A. Samad, G. Brenner, C. J. Woolf, H. Y. Lin, and A. Schneyer. 2005. Localization and action of Dragon (repulsive guidance molecule b), a novel bone morphogenetic protein coreceptor, throughout the reproductive axis. *Endocrinology* 146: 3614–3621.
14. Xia, Y., P. B. Yu, Y. Sidis, H. Beppu, K. D. Bloch, A. L. Schneyer, and H. Y. Lin. 2007. Repulsive guidance molecule RGMa alters utilization of bone morphogenetic protein (BMP) type II receptors by BMP2 and BMP4. *J. Biol. Chem.* 282: 18129–18140.
15. Xia, Y., J. L. Babitt, Y. Sidis, R. T. Chung, and H. Y. Lin. 2008. Hemojuvelin regulates hepcidin expression via a selective subset of BMP ligands and receptors independently of neogenin. *Blood* 111: 5195–5204.
16. Xia, Y., J. L. Babitt, R. Bouley, Y. Zhang, N. Da Silva, S. Chen, Z. Zhuang, T. A. Samad, G. J. Brenner, J. L. Anderson, et al. 2010. Dragon enhances BMP signaling and increases transepithelial resistance in kidney epithelial cells. *J. Am. Soc. Nephrol.* 21: 666–677.
17. Babitt, J. L., Y. Zhang, T. A. Samad, Y. Xia, J. Tang, J. A. Campagna, A. L. Schneyer, C. J. Woolf, and H. Y. Lin. 2005. Repulsive guidance molecule (RGMa), a DRAGON homologue, is a bone morphogenetic protein co-receptor. *J. Biol. Chem.* 280: 29820–29827.
18. Babitt, J. L., F. W. Huang, D. M. Wrighting, Y. Xia, Y. Sidis, T. A. Samad, J. A. Campagna, R. T. Chung, A. L. Schneyer, C. J. Woolf, et al. 2006. Bone morphogenetic protein signaling by hemojuvelin regulates hepcidin expression. *Nat. Genet.* 38: 531–539.
19. Samad, T. A., A. Srinivasan, L. A. Karchewski, S. J. Jeong, J. A. Campagna, R. R. Ji, D. A. Fabrizio, Y. Zhang, H. Y. Lin, E. Bell, and C. J. Woolf. 2004. DRAGON: a member of the repulsive guidance molecule-related family of neuronal- and muscle-expressed membrane proteins is regulated by DRG11 and has neuronal adhesive properties. *J. Neurosci.* 24: 2027–2036.
20. LaPensee, C. R., E. R. Hugo, and N. Ben-Jonathan. 2008. Insulin stimulates interleukin-6 expression and release in LS14 human adipocytes through multiple signaling pathways. *Endocrinology* 149: 5415–5422.
21. Andriopoulos, B., Jr., E. Corradini, Y. Xia, S. A. Faasse, S. Chen, L. Grgurevic, M. D. Knutson, A. Pietrangelo, S. Vukicevic, H. Y. Lin, and J. L. Babitt. 2009. BMP6 is a key endogenous regulator of hepcidin expression and iron metabolism. *Nat. Genet.* 41: 482–487.
22. Niederkofler, V., R. Salie, M. Sigrist, and S. Arber. 2004. Repulsive guidance molecule (RGM) gene function is required for neural tube closure but not retinal topography in the mouse visual system. *J. Neurosci.* 24: 808–818.
23. Cuny, G. D., P. B. Yu, J. K. Laha, X. Xing, J. F. Liu, C. S. Lai, D. Y. Deng, C. Sachidanandan, K. D. Bloch, and R. T. Peterson. 2008. Structure-activity relationship study of bone morphogenetic protein (BMP) signaling inhibitors. *Bioorg. Med. Chem. Lett.* 18: 4388–4392.
24. Yu, P. B., H. Beppu, N. Kawai, E. Li, and K. D. Bloch. 2005. Bone morphogenetic protein (BMP) type II receptor deletion reveals BMP ligand-specific gain of signaling in pulmonary artery smooth muscle cells. *J. Biol. Chem.* 280: 24443–24450.
25. Zhou, Q., J. Heinke, A. Vargas, S. Winnik, T. Krauss, C. Bode, C. Patterson, and M. Moser. 2007. ERK signaling is a central regulator for BMP-4 dependent capillary sprouting. *Cardiovasc. Res.* 76: 390–399.
26. Nojima, J., K. Kanomata, Y. Takada, T. Fukuda, S. Kokabu, S. Ohte, T. Takada, T. Tsukui, T. S. Yamamoto, H. Sasanuma, et al. 2010. Dual roles of smad proteins in the conversion from myoblasts to osteoblastic cells by bone morphogenetic proteins. *J. Biol. Chem.* 285: 15577–15586.
27. Sieber, C., J. Kopf, C. Hiepen, and P. Knaus. 2009. Recent advances in BMP receptor signaling. *Cytokine Growth Factor Rev.* 20: 343–355.
28. Takahashi, M., F. Otsuka, T. Miyoshi, H. Otani, J. Goto, M. Yamashita, T. Ogura, H. Makino, and H. Doihara. 2008. Bone morphogenetic protein 6 (BMP6) and BMP7 inhibit estrogen-induced proliferation of breast cancer cells by suppressing p38 mitogen-activated protein kinase activation. *J. Endocrinol.* 199: 445–455.
29. Yamaguchi, K., S. Nagai, J. Ninomiya-Tsuji, M. Nishita, K. Tamai, K. Irie, N. Ueno, E. Nishida, H. Shibuya, and K. Matsumoto. 1999. XIAP, a cellular member of the inhibitor of apoptosis protein family, links the receptors to TAB1-TAK1 in the BMP signaling pathway. *EMBO J.* 18: 179–187.
30. Wang, P., N. Li, J. S. Li, and W. Q. Li. 2002. The role of endotoxin, TNF-alpha, and IL-6 in inducing the state of growth hormone insensitivity. *World J. Gastroenterol.* 8: 531–536.
31. Lieskovska, J., D. Guo, and E. Derman. 2002. IL-6-overexpression brings about growth impairment potentially through a GH receptor defect. *Growth Horm. IGF Res.* 12: 388–398.
32. Lieskovska, J., D. Guo, and E. Derman. 2003. Growth impairment in IL-6-overexpressing transgenic mice is associated with induction of SOCS3 mRNA. *Growth Horm. IGF Res.* 13: 26–35.